This full text paper was peer reviewed at the direction of IEEE Communications Society subject matter experts for publication in the IEEE Globecom 2011 proceedings.

Time-Frequency Training OFDM with High Spectral Efficiency and Improved Performance over Fast Fading Channels

Linglong Dai, Zhaocheng Wang, Jintao Wang, and Jun Wang
Tsinghua National Laboratory for Information Science and Technology,
Electronic Engineering Department, Tsinghua University, Beijing 10084, China
E-mail: dll07@mails.tsinghua.edu.cn

***Abstract*—Time domain synchronous OFDM (TDS-OFDM) has higher spectral efficiency than cyclic prefix OFDM (CP-OFDM), but suffers from severe performance loss over fast fading channels. In this paper, a novel transmission scheme called time-frequency training OFDM (TFT-OFDM) is proposed. The time-frequency joint channel estimation for TFT-OFDM utilizes the time-domain training sequence without interference cancellation to merely acquire the time delay profile of the channel, while the path coefficients are estimated by using the frequency-domain group pilots. The redundant group pilots only occupy about 1% of the useful subcarriers, thus TFT-OFDM still has much higher spectral efficiency than CP-OFDM by about 10%. Simulation results also demonstrate that TFT-OFDM outperforms CP-OFDM and TDS-OFDM over time-varying channels.**

I. Introduction

OFDM has been widely used in numerous wireless communication systems. There are three fundamental types of OFDM-based block transmission schemes: cyclic prefix OFDM (CP-OFDM) [1], zero padding OFDM (ZP-OFDM) [2], and time domain synchronous OFDM (TDS-OFDM) [3]. The widely used CP-OFDM scheme utilizes the CP to eliminate the inter-block-interference (IBI) as well as inter-carrier-interference (ICI) [4]. The CP is replaced by zero samples in ZP-OFDM to tackle the channel null problem [2]. In TDS-OFDM [3] the known sequence like the pseudorandom noise (PN) sequence is used as the guard interval as well as the training sequence (TS) for synchronization and channel estimation. Consequently, the large amount of frequency-domain pilots used in CP-OFDM and ZP-OFDM can be saved. Thus, TDS-OFDM outperforms CP-OFDM and ZP-OFDM in spectral efficiency by about 10%. As the essential technology, TDS-OFDM has been successfully applied by Chinese national digital television standard [5].

However, the TS and the OFDM data block will cause IBI to each other, and the iterative interference cancellation algorithm with high complexity and poor performance over fading channels has to be used [6]. This issue can be partly solved by inserting redundant pilots to generate the TS in the cyclic postfix OFDM scheme [7], but the inserted pilots suffer from very high average power [8]. The most attractive solution to the interference problem of TDS-OFDM is the dual-PN OFDM (DPN-OFDM) scheme [9], but the double length of the TS leads to the remarkable reduction in spectral efficiency, especially when the guard interval length is long. In summary, it is a big challenge to simultaneously achieve high spectral efficiency as well as good performance over fast fading channels for current OFDM-based transmission schemes.

To solve the challenging problem mentioned above, a novel OFDM transmission scheme called time-frequency training OFDM (TFT-OFDM) is proposed. The innovation and contribution of this paper can be specifically described as below: 1) Unlike CP-OFDM or TDS-OFDM where the training information exists only in the frequency or time domain, TFT-OFDM has TS in the time domain and a very small amount of group pilots in the frequency domain; 2) Unlike CP-OFDM or TDS-OFDM, the proposed time-frequency joint channel estimation in TFT-OFDM utilizes the time-domain TS to merely estimate the time delay profile of the channel, while the path coefficients are acquired by using the frequency-domain group pilots; 3) The group pilots in TFT-OFDM only occupy about 1% of the used subcarriers, thus much higher spectral efficiency than CP-OFDM can be achieved; 4) There is no need to remove the IBI between the TS and OFDM block before channel estimation, thus the iterative interference cancellation algorithm in TDS-OFDM is naturally avoided, leading to the obvious performance improvement over fast fading channels.

The remainder of this paper is organized as follows. The TFT-OFDM system model is described in Section II. The corresponding receiver design is addressed in Section III. Section IV analyzes the spectral efficiency of the proposed scheme. Simulation results are presented in Section V before the final conclusions summarized in Section VI.

Notation: We use the boldface letters to denote matrices and column vectors; $\mathbf{I}_N$ is the $N \times N$ identity matrix, and $\mathbf{0}_{M\times N}$ denotes the $M \times N$ zero matrix; $\mathbf{F}_N$ denotes the normalized $N \times N$ fast Fourier transform (FFT) matrix whose $(n+1, k+1)$th entry being $\exp(-j2\pi nk/N)/\sqrt{N}$; $\otimes$ presents the circular correlation, and $\odot$ means the Hadamard product of two vectors; $(\cdot)^*$, $(\cdot)^{\mathrm{T}}$, $(\cdot)^H$, $(\cdot)^{-1}$ and $|\cdot|$ denote the complex conjugate, transpose, conjugate transpose, matrix inversion and absolute operations, respectively; $\mathrm{diag}\{\mathbf{u}\}$ means a diagonal matrix where the elements of $\mathbf{u}$ are placed at its diagonal positions; $\widehat{x}$ presents the estimate of x.

978-1-4244-9268-8/11/$26.00 ©2011 IEEE

II. System Model of TFT-OFDM

Fig. 1 shows the signal structure comparison between CP-OFDM, TDS-OFDM and the proposed TFT-OFDM schemes.

In the time domain, similar to TDS-OFDM, the ith TFT-OFDM symbol $\mathbf{s}_i = [s_{i,0}\ s_{i,1} \cdots s_{i,P-1}]^T$ is composed of the known TS $\mathbf{c}_i = [c_{i,0}\ c_{i,1} \cdots c_{i,M-1}]^T$ and the OFDM data block $\mathbf{x}_i = [x_{i,0}\ x_{i,1} \cdots x_{i,N-1}]^T$

$$\mathbf{s}_i = \begin{bmatrix} \mathbf{c}_i \\ \mathbf{x}_i \end{bmatrix}_{P\times 1} = \begin{bmatrix} \mathbf{I}_M \\ \mathbf{0}_{N\times M} \end{bmatrix}_{P\times M} \mathbf{c}_i + \begin{bmatrix} \mathbf{0}_{M\times N} \\ \mathbf{I}_N \end{bmatrix}_{P\times N} \mathbf{F}_N^H \mathbf{X}_i, \tag{1}$$

where M is the length of the TS, N is the length of the OFDM data block, $P = M + N$ presents the length of a TFT-OFDM symbol, $\mathbf{X}_i = [X_{i,0}\ X_{i,1} \cdots X_{i,N-1}]^T$ denotes the frequency-domain OFDM symbol, and $\mathbf{x}_i = \mathbf{F}_N^H \mathbf{X}_i$. Being different from the time-domain PN sequence used in TDS-OFDM, the TS in TFT-OFDM could be any kind of sequences with favorable features defined in the time or frequency domain. Here we adopt the TS having constant envelope in the frequency domain, i.e., $\mathbf{c}_i = \mathbf{F}_M^H \mathbf{C}_i$, where $\mathbf{C}_i = [C_{i,0}\ C_{i,1} \cdots C_{i,M-1}]^T$ with the entry $C_{i,k} \in \{+c, -c\}$, and c is an arbitrary real or complex number. For simplicity, $c = 1$ is used. It can be proved that such TS with any length has perfect circular auto-correlation property, since the circular correlation theorem allows

$$\mathbf{c}_i \otimes \mathbf{c}_i = \mathbf{F}_M^H \left(\sqrt{M} \mathbf{F}_M \mathbf{c}_i \odot (\mathbf{F}_M \mathbf{c}_i)^* \right) = M[1\ \mathbf{0}_{1\times(M-1)}]^T. \tag{2}$$

In the frequency domain, unlike TDS-OFDM where all active subcarriers are used to carry data, TFT-OFDM has N_d data subcarriers and N_{group} group pilots scattered within the signal bandwidth. Each group has $2d+1$ pilots. The index set of the central pilot within each group can be denoted by $\boldsymbol{\eta} = \{\eta_0\ \eta_1 \cdots \eta_{N_{group}-1}\}$, and the index set of all pilots is $\boldsymbol{\Psi} = \{\eta_0 - d\ \eta_0 - d + 1 \cdots \eta_0 + d \cdots \eta_{N_{group}-1} - d \cdots \eta_{N_{group}-1} + d\}$, and the pilot number is $N_p = N_{group}(2d+1)$, where $N = N_d + N_p$. Later in Section III-A, we will show that TFT-OFDM requires much smaller amount of pilots than CP-OFDM.

After the cyclic reconstruction of the received OFDM block has been achieved (the specific method will be addressed in Section III-B), the received frequency-domain OFDM block $\mathbf{Y}_i = [Y_{i,0}, Y_{i,1}, \cdots Y_{i,N-1}]^T$ can be expressed as

$$\mathbf{Y}_i = \mathbf{H}_i \mathbf{X}_i + \mathbf{W}_i, \tag{3}$$

where $\mathbf{W}_i$ is the additive white Gaussian noise (AWGN) vector with each element having zero mean and the variance of σ^2, $\mathbf{H}_i$ is the channel frequency response (CFR) matrix with the $(p+1, q+1)$th entry $H_{i,p,q}$ be [10]

$$H_{i,p,q} = \sum_{l=0}^{L-1} \left(\frac{1}{N} \sum_{n=0}^{N-1} h_{i,n,l} e^{-j\frac{2\pi}{N} n(p-q)} \right) e^{-j\frac{2\pi}{N} q n_l}, \tag{4}$$

where $h_{i,n,l}$ denotes the coefficient of the lth path with the delay of n_l at the time instant of n within the ith OFDM block, L is the number of resolvable paths. If the channel is time-invariant within each TFT-OFDM symbol, i.e., $h_{i,0,l} = h_{i,1,l} = \cdots = h_{i,N-1,l} = h_{i,l}$, the ICI coefficient $H_{i,p,q}$ $(p \neq q)$ is zero, and $\mathbf{H}_i$ becomes a diagonal matrix.

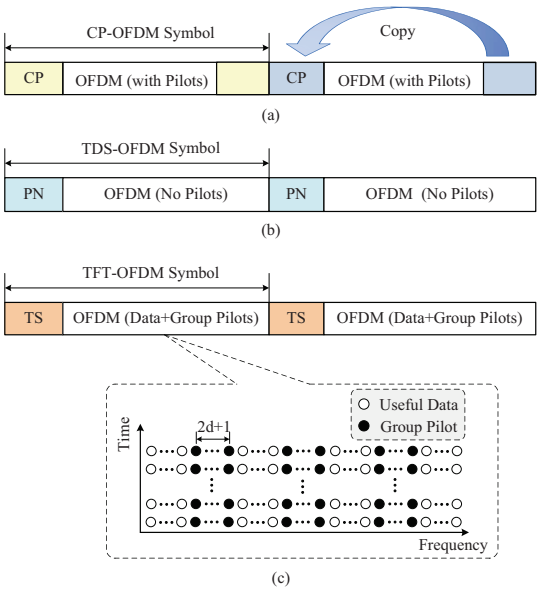

Fig. 1. Signal structure comparison between CP-OFDM, TDS-OFDM and the proposed TFT-OFDM: (a) CP-OFDM; (b) TDS-OFDM; (c) TFT-OFDM.

III. TFT-OFDM Receiver Design

This section presents the TFT-OFDM receiver design issues, including the time-frequency joint channel estimation, cyclic prefix reconstruction and channel equalization.

A. Time-Frequency Joint Channel Estimation

Unlike CP-OFDM or TDS-OFDM where channel estimation is solely dependent on the frequency-domain pilots or the time-domain TS, channel estimation in TFT-OFDM is jointly achieved by time-frequency processing of the received TFT-OFDM signal.

1) Time Delay Profile Estimation Using Time-Domain TS

For simplicity, we firstly assume that the channel is time-invariant during one TFT-OFDM symbol. Let $\mathbf{h}_i = [h_{i,0}\ h_{i,1} \cdots h_{i,L-1}]^T$ be the channel impulse response (CIR) vector, the received TS $\mathbf{d}_i = [d_{i,0}\ d_{i,1} \cdots d_{i,M-1}]^T$ should be

$$\mathbf{d}_i = \mathbf{B}_{i,\mathrm{ISI}} \mathbf{c}_i + \mathbf{B}_{i-1,\mathrm{IBI}} \mathbf{x}_{i-1,N-M:N-1} + \mathbf{v}_i, \tag{5}$$

where $\mathbf{B}_{i,\mathrm{ISI}}$ denotes the $M \times M$ Toeplitz inferior triangular matrix with the first column $[h_{i,0}\ h_{i,1} \cdots h_{i,L-1}\ 0 \cdots 0]^T$, $\mathbf{B}_{i,\mathrm{IBI}}$ presents the $M \times M$ Toeplitz superior triangular matrix of the first row $[0 \cdots 0\ h_{i,L-1}\ h_{i,L-2} \cdots h_{i,1}]^T$, $\mathbf{x}_{i-1,N-M:N-1}$ denotes the last M elements of $\mathbf{x}_{i-1}$, and $\mathbf{B}_{i,\mathrm{IBI}} \mathbf{x}_{i-1,N-M:N-1}$ is the interference caused by the previous OFDM block $\mathbf{x}_{i-1}$, $\mathbf{v}_i$ is the AWGN vector.

In TDS-OFDM, the interference $\mathbf{B}_{i,\mathrm{IBI}} \mathbf{x}_{i-1,N-M:N-1}$ must be cancelled [6], which is difficult even if the CIR is exactly known, since $\mathbf{x}_{i-1}$ is random and cannot be perfectly detected. Therefore, performance loss is unavoidable, especially when the channel is varying fast. To solve this problem, without interference cancellation, we directly use the "contaminated"

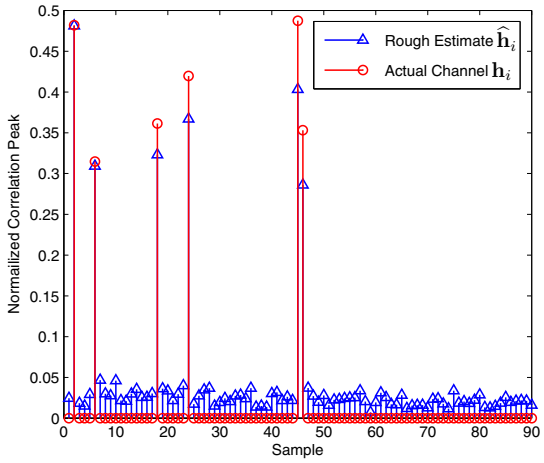

Fig. 2. Time delay profile estimation using the time-domain TS without interference cancellation and cyclic prefix reconstruction.

TS to only estimate the time delay profile of the CIR

$$\widehat{\mathbf{h}}_i = \frac{1}{M}\mathbf{c}_i \otimes \mathbf{d}_i = \mathbf{h}_i + \mathbf{v}_i{}' + \mathbf{n}_i, \tag{6}$$

where $\mathbf{v}_i{}' = \frac{1}{M}\mathbf{c}_i \otimes \mathbf{v}_i$ is the noise term, and

$$\mathbf{n}_i = \frac{1}{M}\mathbf{c}_i \otimes (\mathbf{B}_{i-1,\mathrm{IBI}}\mathbf{x}_{i-1,N-M:N-1} - \mathbf{B}_{i,\mathrm{IBI}}\mathbf{c}_i) \tag{7}$$

denotes the extra "noise" due to the interference. However, $\mathbf{n}_i$ will not severely affect the time delay information of the channel, since $\mathbf{x}_{i-1}$ and $\mathbf{c}_i$ are completely uncorrelated. As an example, Fig. 2 compares $\widehat{\mathbf{h}}_i$ and $\mathbf{h}_i$ over the Brazil D channel with the signal-to-noise ratio (SNR) of 5 dB. Although the rough estimate $\widehat{\mathbf{h}}_i$ is not accurate due to the interference, the time delay profile of the channel is preserved well, as demonstrated in Fig. 2, which is just the expected target of this stage. Moreover, $\widehat{\mathbf{h}}_i$ can be further refined by averaging several results from (6). Finally, the time delays of the most significant taps of $\widehat{\mathbf{h}}_i$ are saved in the time delay profile set $\mathbf{\Gamma}$

$$\mathbf{\Gamma} = \{n_l : \left|\widehat{h}_{i,l}\right|^2 \geq P_{th}\}_{l=0}^{L-1}, \tag{8}$$

where P_{th} is pre-defined power threshold.

2) Path Coefficient Estimation Using Frequency-domain Pilots

For time-varying channels, the path coefficient $h_{i,n,l}$ in (4) can be modeled by the Q-order Taylor series expansion [11]

$$h_{i,n,l} = \boldsymbol{\theta}_n \boldsymbol{\rho}_{i,l} + \varepsilon_{i,n,l}, \tag{9}$$

where $\boldsymbol{\theta}_n = [1 \ n \ n^2 \cdots n^Q]_{1\times(Q+1)}$, $\boldsymbol{\rho}_{i,l} = [\rho_{i,l,0} \ \rho_{i,l,1} \cdots \rho_{i,l,Q}]^T_{(Q+1)\times 1}$, $\rho_{i,l,q}$ is the polynomial coefficient, and $\varepsilon_{i,n,l}$ denotes the approximation error. The order Q depends on the maximum Doppler spread f_d of the channel. According to the study in [11], $Q = 1$ ensures good approximation performance if $f_d T \leq 0.1$, where T is the OFDM block length. Take the value $T = 500\mu s$ specified in [5] as an example, $f_d \leq 200$ Hz meets such criterion.

Since the ICI is dominantly caused by the neighboring subcarriers [11], it can be assumed that the ICI coefficient $H_{i,p,q} = 0$ if $|p-q| > d$. Thus, by substituting (9) and (4) into (3), $Y_{i,k}$ can be rewritten as

$$Y_{i,k} = \mathbf{\Lambda}_{i,k}\boldsymbol{\theta}_i\boldsymbol{\rho}_i + \zeta_{i,k}, \tag{10}$$

where $\mathbf{\Lambda}_{i,k} = [\lambda_{i,0,0,k} \ \lambda_{i,0,1,k} \cdots \lambda_{i,N-1,L-1,k}]_{1\times LN}$ with

$$\lambda_{i,n,l,k} = \frac{1}{N}\sum_{q=k-d}^{k+d} e^{-j\frac{2\pi}{N}n(k-q)} e^{-j\frac{2\pi}{N}qn_l} X_{i,q}, \tag{11}$$

$\boldsymbol{\theta}_i = [\boldsymbol{\theta}_{i,0}^T \ \boldsymbol{\theta}_{i,1}^T \ \boldsymbol{\theta}_{i,2}^T \cdots \boldsymbol{\theta}_{i,N-1}^T]^T_{NL\times(Q+1)L}$ with the entry $\boldsymbol{\theta}_{i,n} = [diag\{\boldsymbol{\theta}_n \ \boldsymbol{\theta}_n \ \boldsymbol{\theta}_n \cdots \boldsymbol{\theta}_n\}]_{L\times(Q+1)L}$, $\boldsymbol{\rho}_i = [\boldsymbol{\rho}_{i,0}^T \ \boldsymbol{\rho}_{i,1}^T \cdots \boldsymbol{\rho}_{i,L-1}^T]^T_{(Q+1)L\times 1}$, and the noise term $\zeta_{i,k} = \sum_{n=0}^{N-1}\sum_{l=0}^{L-1} \varepsilon_{i,n,l}\lambda_{i,n,l,k} + W_{i,k}$.

Using the known group pilots $\{X_{i,q}\}_{q=k-d}^{k+d}$ and the time delay profile $\mathbf{\Gamma}=\{n_l\}_{l=0}^{L-1}$ in (8), $\lambda_{i,n,l,k}$ in (11) can be calculated if $k \in \boldsymbol{\eta}$, and $\mathbf{\Lambda}_i=[\mathbf{\Lambda}_{i,\eta_0}, \mathbf{\Lambda}_{i,\eta_1}, \cdots \mathbf{\Lambda}_{i,\eta_{N_{group}-1}}]^T_{N_{group}\times LN}$ is consequently known. Therefore, the received central pilots in the frequency-domain group pilots in (10), i.e., $\mathbf{Y}_p = [Y_{i,\eta_0} \ Y_{i,\eta_1} \cdots Y_{i,\eta_{N_{group}-1}}]^T_{N_{group}\times 1}$, can be expressed by

$$\mathbf{Y}_p = \mathbf{\Lambda}_i\boldsymbol{\theta}_i\boldsymbol{\rho}_i + \boldsymbol{\zeta}_i, \tag{12}$$

where $\boldsymbol{\zeta}_i = [\zeta_{i,\eta_0} \ \zeta_{i,\eta_1} \cdots \zeta_{i,\eta_{N_{group}-1}}]^T_{N_{group}\times 1}$.

Because $\boldsymbol{\rho}_i$ in (12) contains $(Q+1)L$ unknown parameters, the number of group pilots should satisfy $N_{group} \geq (Q+1)L$ to guarantee the matrix $\boldsymbol{\beta}_i = \mathbf{\Lambda}_i\boldsymbol{\theta}_i$ to be of full column rank. Thus, $\boldsymbol{\rho}_i$ can be estimated as

$$\widehat{\boldsymbol{\rho}}_i = \boldsymbol{\beta}_i^{\dagger}\mathbf{Y}_p = \left(\boldsymbol{\beta}_i^H\boldsymbol{\beta}_i\right)^{-1}\boldsymbol{\beta}_i^H\mathbf{Y}_p, \tag{13}$$

where $(\cdot)^{\dagger}$ denotes the Moore-Penrose inverse matrix. Then, $h_{i,n,l}$ in (9) and $H_{i,p,q}$ in (4) can be calculated based on $\widehat{\boldsymbol{\rho}}_i$.

Note that only $N_p = (Q+1)(2d+1)L$ pilots are required in TFT-OFDM to estimate the path coefficients after the time delay profile has been known according to (8). In addition, it has been shown that $Q = 1, d = 1$ can already provide satisfying performance over fading channels [11], so the pilot number N_p is small. However, both the time delays and path coefficients are estimated by using the frequency-domain pilots in CP-OFDM, and the pilot number should be not smaller than the CP length M according to the Karhunen-Loeve theorem [10]. Therefore, TFT-OFDM needs much fewer pilots than CP-OFDM due to L is normally much smaller than M, i.e., $L \ll M$.

B. Channel Equalization

Due to the multi-path propagation, the received OFDM block $\mathbf{y}_i = [y_{i,0} \ y_{i,1} \cdots y_{i,N-1}]^T$ can be expressed by

$$\mathbf{y}_i = \mathbf{H}_{i,\mathrm{ISI}}\mathbf{x}_i + \mathbf{H}_{i,\mathrm{IBI}}\begin{bmatrix} \mathbf{0}_{(N-M)\times 1} \\ \mathbf{c}_i \end{bmatrix}_{N\times 1} + \mathbf{w}_i, \tag{14}$$

where $\mathbf{H}_{i,\mathrm{ISI}}$ and $\mathbf{H}_{i,\mathrm{IBI}}$ be the $N \times N$ Toeplitz inferior and superior triangular matrix with the first column $[h_{i,0} \ h_{i,1} \cdots h_{i,L-1} \ 0 \cdots 0]^T$ and the first row $[0 \cdots 0 \ h_{i,L-1} \ h_{i,L-2} \cdots h_{i,1}]^T$, respectively, and $\mathbf{w}_i = \mathbf{F}_N^H\mathbf{W}_i$ is the AWGN vector. Similar to the hybrid domain

equalization method proposed in [12], cyclic prefix reconstruction of $\mathbf{y}_i$ can be achieved by

$$\begin{aligned}\widetilde{\mathbf{y}}_i &= \mathbf{y}_i - \mathbf{H}_{i,\mathrm{IBI}}\begin{bmatrix}\mathbf{0}_{(N-M)\times 1}\\ \mathbf{c}_i\end{bmatrix}_{N\times 1} + \begin{bmatrix}\mathbf{d}_{i+1}\\ \mathbf{0}_{(N-M)\times 1}\end{bmatrix} - \mathbf{H}_{i,\mathrm{ISI}}\begin{bmatrix}\mathbf{c}_{i+1}\\ \mathbf{0}_{(N-M)\times 1}\end{bmatrix}\\ &= \mathbf{H}_{i,\mathrm{CIR}}\mathbf{x}_i + \mathbf{w}_i + \begin{bmatrix}\mathbf{v}_{i+1}\\ \mathbf{0}_{(N-M)\times 1}\end{bmatrix}. \qquad (15)\end{aligned}$$

where $\mathbf{d}_{i+1}$ can be found according to (5), and $\mathbf{H}_{i,\mathrm{CIR}} = \mathbf{H}_{i,\mathrm{ISI}} + \mathbf{H}_{i,\mathrm{IBI}}$ means the $N \times N$ circular matrix with the first column $[h_{i,0}\ h_{i,1}\cdots h_{i,L-1}\ 0\cdots 0]^T$. Since any circular matrix can be diagonalized by the FFT matrix, i.e., $\mathbf{H}_{i,\mathrm{CIR}} = \mathbf{F}_N\mathbf{H}_i\mathbf{F}_N^H$, applying DFT to $\widetilde{\mathbf{y}}_i$ would produce the signal $\mathbf{Y}_i$ in (3), i.e., $\mathbf{Y}_i = \mathbf{F}_N\widetilde{\mathbf{y}}_i = \mathbf{H}_i\mathbf{X}_i + \mathbf{W}_i$.

Then, the zero-forcing equalization can be performed after the iterative ICI removal:

- *Step 1: Initial channel equalization*. The CFR estimate $\widehat{H}_{i,p,q}$ in (4) can be calculated after channel estimation. Then the initial channel equalization is performed as

$$\widehat{X}_{i,k}^{(0)} = \frac{Y_{i,k}}{\widehat{H}_{i,k,k}},\ k \notin \mathbf{\Psi}. \qquad (16)$$

- *Step 2: Iterative ICI cancellation*. Since the ICI is dominantly caused by the adjacent subcarriers, the transmitted signal on the kth subcarrier in the jth iteration is updated according to

$$\widehat{X}_{i,k}^{(j)} = \frac{Y_{i,k} - \sum_{q=k-d,q\neq k}^{k+d}\widehat{H}_{i,k,q}\widehat{X}_{i,q}^{(j-1)}}{\widehat{H}_{i,k,k}},\ k \notin \mathbf{\Psi}. \qquad (17)$$

- *Step 3: Iteration termination*. The iterative process is stopped if the pre-defined iteration number J_0 (normally $J_0 \leq 3$) is approached. Otherwise, jump to *Step 2*.

Note that the channel equalization and estimation in TFT-OFDM are not iteratively performed like that in TDS-OFDM.

IV. Spectral Efficiency of TFT-OFDM

A. Spectral Efficiency

Both the time-domain guard interval and the frequency-domain pilots are the overheads for OFDM systems [13]. So the spectral efficiency of TFT-OFDM is

$$\mathrm{E}_0 = \frac{N-(Q+1)(2d+1)L}{M+N}. \qquad (18)$$

Table I shows the spectral efficiency comparison between CP-OFDM, TDS-OFDM, DPN-OFDM and the proposed TFT-OFDM. For digital broadcasting systems, typically $N = 4096$ is selected. In addition, all the channel models defined by ITU have not more than 6 resolvable paths, so we assumed $L = 6$ without the loss of generality, and $Q = 1, d = 1$ are considered as mentioned before. In this case, only 36 pilots occupying less than 1% of the used subcarriers in TFT-OFDM, is sufficient to track the time-varying channel, while CP-OFDM requires 12.5% pilot occupation ratio when $M = N/8$.

It is clear from Table I that TFT-OFDM only suffers from negligible loss in spectral efficiency compared with TDS-OFDM who has the least overhead. It also shows that TFT-OFDM has higher efficiency than CP-OFDM and DPN-OFDM, especially when the guard interval is long, which is just the important application scenario of single frequency network (SFN) mode for the digital broadcasting systems as well as the next generation wireless system called the long term evolution (LTE) [14]. For example, TFT-OFDM has higher spectral efficiency than CP-OFDM by about 9.74% when $M = N/8$, and TFT-OFDM outperforms DPN-OFDM by the increase of 12.63% in spectral efficiency when $M = N/4$.

TABLE I
Spectral efficiency comparison.

TS Length	CP-OFDM	TDS-OFDM	DPN-OFDM	TFT-OFDM
$K = N/4$	60.00%	80.00%	66.67%	79.30%
$K = N/8$	77.78%	88.89%	80.00%	87.52%
$K = N/16$	88.23%	94.12%	88.89%	92.59%

B. Extension to Multiple-Input Multiple-Output (MIMO) Scenarios

It is well-known that extending TDS-OFDM to MIMO applications is difficult due to the much more complicated interference issue than that in the single-antenna TDS-OFDM system [15]. CP-OFDM can be easily extended to MIMO systems by adopting orthogonal pilots, at the high cost of the linearly increased pilots with respect to the transmit antenna number N_T[1]. However, without the obvious increase in the overhead, the proposed TFT-OFDM can be easily adapted to MIMO scenarios by configuring quasi-orthogonal time-domain TS to each transmit antenna, and using orthogonal pilots in the frequency domain. Taking $N = 4096, M = N/8, N_p = 36, N_T = 4$ as an example, we can find that 50% of the used subcarriers would be occupied by the pilots in CP-OFDM-MIMO, while the group pilots in TFT-OFDM-MIMO take up only 3.5% of the signal bandwidth.

V. Simulation Results and Discussion

Simulations were carried out to investigate the performance of the proposed TFT-OFDM transmission scheme. The signal bandwidth is 7.56 MHz at the central radio frequency of 770 MHz. The modulation scheme is QPSK. Other system parameters are consistent with those specified in Section IV-A. Two typical 6-tap multi-path channel models named Vehicular B and Brazil D were used. The first channel has moderate frequency-selectivity, while the later has deep frequency-selectivity. The maximum Doppler spread of 20 Hz and 100 Hz are considered, which correspond to the relative receiver velocity of 28 km/h and 140 km/h @ 770 MHz, respectively.

Fig. 3 compares the bit error rate (BER) performance of TFT-OFDM with CP-OFDM, TDS-OFDM and DPN-OFDM over the Vehicular B channel with the receiver velocity of 28 km/h. In CP-OFDM, the comb-type pilots were used for least square channel estimation, and then discrete Fourier transform interpolation was used [1]. We can observe that TFT-OFDM has superior BER performance over the conventional OFDM transmission schemes. When BER is 0.1, TFT-OFDM outperforms DPN-OFDM, CP-OFDM and TDS-OFDM by about 0.6 dB, 1.5 dB and 3.1 dB, respectively.

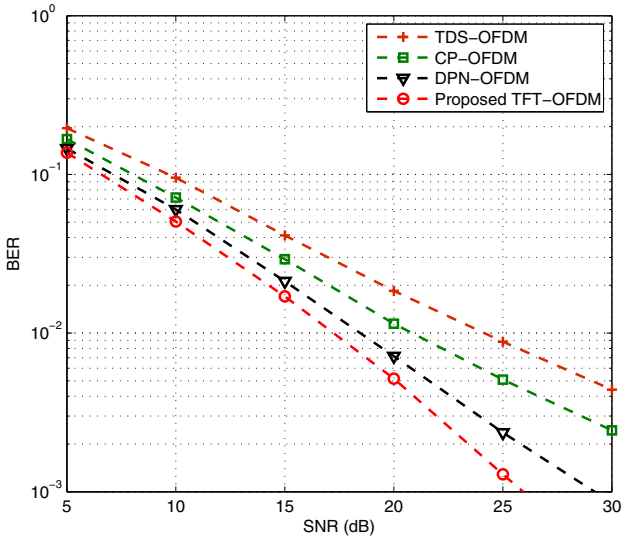

Fig. 3. BER performance comparison between the proposed TFT-OFDM scheme and three traditional schemes over the Vehicular B channel with the receiver velocity of 28 km/h.

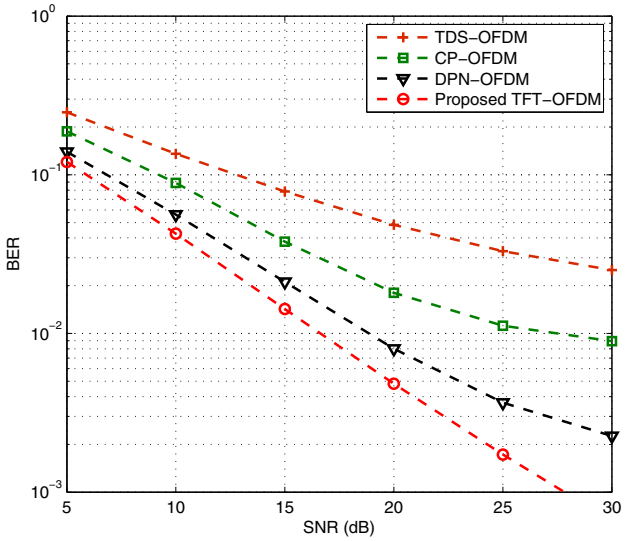

Fig. 4. BER performance comparison between the proposed TFT-OFDM scheme and three traditional schemes over the Brazil D channel with the receiver velocity of 140 km/h.

Fig. 4 shows the BER performance comparison of those four OFDM-based transmission schemes over the Brazil D channel with the mobile speed of 140 km/h. It can be observed that TFT-OFDM still has the best performance, and the advantage has been enlarged over the fast fading channel. For example, when the BER equals to 0.1, compared with DPN-OFDM, CP-OFDM and TDS-OFDM, the SNR gain achieved by TFT-OFDM is increased to be about 1.0 dB, 3.3 dB and 6.9 dB, respectively. The superior performance of TFT-OFDM over TDS-OFDM is mainly contributed by the avoidance of the conventional iterative interference cancellation algorithm with poor performance over fast time-varying channels. Compared with CP-OFDM and DPN-OFDM, TFT-OFDM achieves the performance improvement due to the proposed joint channel estimation can accurately track the channel variation, and ICI is removed before the frequency-domain equalization.

VI. Conclusions

This paper proposed a novel OFDM-based transmission scheme called TFT-OFDM, where the training information exists both in the time and frequency domains. The corresponding time-frequency joint channel estimation naturally avoids the conventional iterative interference cancellation algorithm with high complexity and poor performance. It also it tracks the variation of the fading channels well and ICI is removed to further improve the system performance. The group pilots in TFT-OFDM occupy only about 1% of the signal bandwidth. Therefore, high spectral efficiency as well as good performance over fast time-varying channels can be simultaneously achieved. In addition, TFT-OFDM can be easily extended to MIMO and multiple access scenarios without obvious increase in the overhead.

Acknowledgments

This work was supported by Standardization Administration of the People's Republic of China with No. 200910244, and by a grant from the Ph.D. Programs Foundation of Ministry of Education of China with No. 20090002120026.

References

[1] L. Hanzo, M. Munster, B. J. Choi, and T. Keller, *OFDM and MC-CDMA for Broadband Multi-User Communications, WLANs and Broadcasting*. Chichester, UK: John Wiley, 2003.

[2] B. Muquet, Z. Wang, G. B. Giannakis, M. de Courville, and P. Duhamel, "Cyclic prefix or zero-padding for multi-carrier transmissions?" *IEEE Trans. Commun.*, vol. 50, no. 12, pp. 2136–2148, Dec. 2002.

[3] C. yen Ong, J. Song, C. Pan, and Y. Li, "Technology and standards of digital television terrestrial multimedia broadcasting," *IEEE Commun. Mag.*, vol. 48, no. 5, pp. 119–127, May 2010.

[4] L. Dai, J. Wang, Z. Wang, J. Wang, and Z. Yang, "Pilot design and channel estimation for TDS-OFDM system with transmit diversity," *IEICE Trans. Commun.*, vol. E94-B, no. 3, pp. 852–855, Mar. 2011.

[5] *Framing Structure, Channel Coding and Modulation for Digital Television Terrestrial Broadcasting System*. Chinese National Standard, GB 20600-2006, Aug. 2006.

[6] J. Wang, Z. Yang, C. Pan, and J. Song, "Iterative padding subtraction of the PN sequence for the TDS-OFDM over broadcast channels," *IEEE Trans. Consumer Electron.*, vol. 51, no. 11, pp. 1148–1152, Nov. 2005.

[7] J. Kim, S. Lee, and J. Seo, "Synchronization and channel estimation in cyclic postfix based OFDM systems," *IEICE Trans. Commun.*, vol. E90-B, no. 3, pp. 485–490, Mar. 2007.

[8] M. Huemer, Ch. Hofbauer, and J. B. Huber, "Unique word prefix in SC/FDE and OFDM: a comparison," in *Proc. IEEE GLOBECOM'2010* (Miami, USA), Dec. 2010, pp. 1321–1326,

[9] J. Fu, J. Wang, J. Song, J, C. Pan, and Z. Yang, "A simplified equalization method for dual PN-sequence padding TDS-OFDM systems," *IEEE Trans. Broadcast.*, vol. 54, no. 4, pp. 825–830, Dec. 2008.

[10] W.-G. Song and J.-T. Lim, "Channel estimation and signal detection for MIMO-OFDM with time varying channels," *IEEE Commun. Lett.*, vol. 10, no. 7, pp. 540–542, Jul. 2006.

[11] Z. Tang, R. C. Cannizzaro, G. Leus, and P. Banelli, "Pilot-assisted time-varying channel estimation for OFDM systems," *IEEE Trans. Signal Processing*, vol. 55, no. 5, pp. 2226–2238, May 2007.

[12] X. Wang, H. Li, and H. Lin, "A new adaptive OFDM system with precoded cyclic prefix for dynamic cognitive radio communications," *IEEE J. Select. Areas Commun.*, vol. 29, no. 2, pp. 431–442, Feb. 2011.

[13] Z. Yang, L. Dai, J. Wang, and Z. Wang, "Transmit diversity for TDS-OFDM broadcasting system over doubly selective fading channels,", *IEEE Trans. Broadcast.*, vol. 57, no. 1, pp. 135–142, Mar. 2011.

[14] S. Sesia, I. Toufik, and M. Baker, *LTE-The UMTS Long Term Evolution: From Theory to Practice*. New Jersey, SA: John Wiley & Sons, 2009.

[15] L. Dai, Z. Wang, and S. Chen, "A novel uplink multiple access scheme based on TDS-FDMA," *IEEE Trans. Wireless Commun.*, vol. 10, no. 3, pp. 757–761, Mar. 2011.